Journal of Luminescence 186 (2017) 312–317

Contents lists available at ScienceDirect

Journal of Luminescence

journal homepage: www.elsevier.com/locate/jlumin

Luminescence and carrier dynamics in nanostructured silicon

Neil Irvin Cabello [a,*], Philippe Tingzon [a,b], Kerr Cervantes [a], Arven Cafe [a], Joybelle Lopez [a,b], Arvin Mabilangan [a], Alexander De Los Reyes [a], Lorenzo Lopez Jr. [a,b], Joselito Muldera [d], Dinh Cong Nguyen [c], Xuan Tu Nguyen [c], Hong Minh Pham [c], Thanh Binh Nguyen [c], Arnel Salvador [a,b], Armando Somintac [a,b], Elmer Estacio [a,b]

[a] Condensed Matter Physics Laboratory, National Institute of Physics, University of the Philippines, Diliman, Quezon City 1101, Philippines
[b] Materials Science and Engineering Program, University of the Philippines, Diliman, Quezon City 1101, Philippines
[c] Institute of Physics, Vietnam Academy of Science and Technology, 10 Dao Tan, Ba Dinh, Hanoi, Vietnam
[d] De La Salle University, 2401 Taft Avenue, Manila 1004, Philippines

ARTICLE INFO

Article history:
Received 14 October 2016
Received in revised form
16 January 2017
Accepted 5 February 2017
Available online 7 February 2017

Keywords:
Nanostructures
Time-resolved photoluminescence
Carrier dynamics

ABSTRACT

We report increased radiation in the visible and terahertz (THz) regimes in silicon(Si)-based nanostructures. The nanostructures, Si nanowires (SiNWs) and porous Si (PSi), were synthesized via electroless and electrochemical surface modification, respectively. In particular, picosecond (ps) radiative lifetimes in the order of 250 ps were obtained from time-resolved photoluminescence (PL) measurements. The fast radiative lifetimes are associated with increased surface defect density in PSi. Reflectance measurements confirmed that optical absorption of the nanostructured Si samples increased relative to bulk Si. Both nanostructured Si exhibit THz emission, albeit weaker in PSi due to higher density of defects. An inverse relationship between PL and THz emission strength was therefore observed. Lastly, the wider bandwidth of the THz emission in SiNWs is attributed to the directionality of the transient photocurrent compared to the more disordered carrier transport in PSi.

1. Introduction

Among the most widely used semiconductor material in electronics and photovoltaics has been silicon (Si) due to its low cost and abundance. Its dominant market share in the semiconductor industry is evidenced by mature Si technology. Aside from photovoltaics however, the photonic and optoelectronic applications of Si are limited due to its indirect band gap and low electron mobility [1].

A possible way to improve Si's photovoltaic efficiency is by surface modification through formation of nanostructures. These nanostructured Si (nanoSi) are of great interest since they have novel or enhanced properties compared to their bulk parent material [2,3]. In particular, the two types of nanoSi that were studied in this report are porous Si (PSi) and Si nanowires (SiNWs).

The PSi is a sponge-like form of Si. The Si structures in between the pores have nanometer dimensions, and are characterized by a high degree of disorder due to effects such as pore side branching [3]. It has been reported to have visible room temperature photoluminescence (PL) [2]. The origin of this PL has been attributed to either quantum confinenement [2] or the presence of surface defect states [4], as Si is not expected to have intense excitonic optical emission due to its indirect band gap. The SiNWs are small scaled, one-dimensional form of Si, and have also been reported to exhibit PL similar to PSi [5–7]. Both forms of nanoSi have promising applications such as drug delivery [8,9], antibacterial agents [10,11], and photocatalysts [12,13] due to their reduced dimensions. Moreover, these nanoSi structures have been reported to possess greatly improved light absorption capabilities compared to bulk Si [14–17]. Due to its structural difference and reduced dimensions compared with bulk Si, nanoSi may also have different carrier transport characteristics [18–20].

As both optical properties and carrier transport play an important role in the performance of optoelectronic devices and solar cells, investigating the optical properties in the framework of studying photogenerated carrier dynamics may lead to improved growth and design of in these novel Si-based devices. For example, high light absorption, low surface recombination and efficient carrier transport are desired for photovoltaic applications [21]. The study and understanding of nanoSi photocarrier transport and recombination properties would be of great help in improving the performance of future nanoSi-based optical and optoelectronic devices.

2. Methodology

All Si wafers used for this work were p $^{+}$-doped with resistivity of 0.007–0.025 Ω cm^2 and crystal orientation of (100), and all

* Corresponding author.
E-mail address: ncabello@nip.upd.edu.ph (N.I. Cabello).

http://dx.doi.org/10.1016/j.jlumin.2017.02.012
0022-2313/

nanoSi synthesis were done under ambient room temperature of 25.0 °C. Standard degreasing procedures were used to clean the wafers. Parts of the wafers were cleaved to sizes of 1.00×1.75 cm^2, which was used to produce the PSi samples. PSi etching was performed using a standard lateral electrochemical etching setup, with 1.0×1.0 cm^2 of the Si chip submerged. The electrochemical etching solution was composed of 1:1 volumetric ratio of 12% HF and absolute ethanol. One set of samples was etched at 3 mA to obtain low-porosity PSi. The second set of samples was etched at 30 mA to obtain high-porosity PSi. For both sets, the etch times were varied to obtain pore depths of 1 μm, 2 μm and 3 μm. All PSi samples were rinsed with ethanol and allowed to dry under ambient conditions. From previous reflectance spectroscopy and Bruggeman effective mass approximation [22], the porosity of each sample set was determined to be 52% and 73% for the low-porosity and high-porosity sample sets, respectively. For convenience, the low-porosity and the high-porosity sample sets shall be labelled as PSi Lo and PSi Hi, respectively. Parts of the wafer were also cleaved to 1.0×1.0 cm^2 sizes to be used for SiNW formation. The cleaved Si were immersed in a solution containing 5.0 M HF and 0.02 M $AgNO_3$ to etch the NWs. The etch times used were 10 min, 20 min and 30 min to produce 1 μm, 2 μm and 3 μm NWs, respectively. The formed Ag dendrites were then removed by immersing the samples in 3:1 volumetric ratio of range 28–30% NH_4OH and 30% H_2O_2 for two minutes. The samples were then rinsed with deionized water and were then allowed to dry in ambient room conditions. Representative SEM images of the nanoSi samples are shown in Fig. 1.

The optical properties of the samples were initially investigated using normal incidence reflectance spectroscopy with scan range from range 1.13 to 2.75 eV. A 10 W tungsten halogen lamp dispersed by a SPEX 500 M monochromator was used as the excitation source. A silicon photodiode was used to detect the reflectance signal. Standard lock-in techniques were employed for data acquisition.

Time-integrated PL spectroscopy was carried out using a 488 nm Ar^+ laser for excitation, which was incident on the sample at an oblique angle. Appropriate optics were used to collect the PL signal. The PL was dispersed and detected by a SPEX 500 M spectrometer fitted with a Hamamatsu R636 GaAs photomultiplier tube. Temperature-dependent PL spectroscopy was done by mounting the samples on a closed-cycle helium cryostat. NanoSi samples exhibiting intense PL were chosen for further luminescence measurements. The time-resolved PL data of the samples were then taken for samples exhibiting intense PL. A 405 nm picosecond pulsed diode laser operating at 4 MHz frequency and having a pulse width of 50 ps was split into two by a beam splitter. One beam was used as PL excitation for the sample. The other beam was directed to a fast photodiode connected to a PicoHarp 300 time-correlated single photon counting system to trigger the data acquisition in a photomultiplier tube and obtain the temporal profile of the PL. The PL was dispersed and detected by a Cornerstone 260 spectrometer equipped with a Hamamatsu R3808-50 microchannel plate photomultiplier tube.

The THz emission of the samples were obtained by using a standard THz-TDS spectroscopy setup in the reflection excitation geometry. The excitation was provided by a mode-locked Ti:sapphire laser generating 100 fs pulses with wavelength centered at 800 nm and with a repetition rate of 80 MHz. The beam was split into a pump arm and a probe arm. The pump beam was used to excite the sample, and the THz emission of the sample was collected in specular reflection direction using appropriate paraboloid mirrors. The THz pulse was detected in the time domain using a LT-GaAs photoconductive dipole antenna, which was optically trigerred by the time-delayed probe beam.

3. Results and discussion

To observe differences in the optical properties of the nanoSi samples, normal incidence reflectance spectra of representative nanoSi samples were taken. Fig. 2 shows the representative reflectance spectra of samples with 1 μm PSi pore depths and 1 μm SiNW thickness. It can be seen that there is a drastic reduction in the reflectance of the nanoSi samples compared with that of the bulk Si. The peak photon energy of the THz-TDS excitation, PL excitation beam and the samples' luminescence peak are indicated by vertical lines to establish the relative absorption properties of the samples at each pertinent energy.

The reduced reflectance may be ascribed to improved light trapping by multiple reflections within the samples [23], which should result to improved photocarrier generation in both PSi and SiNW samples. The marked difference in the absorption characteristics, specifically at the key photon energy values corresponding to the excitation for the THz-TDS and time-integrated PL spectroscopy implies higher signal levels in both measurements.

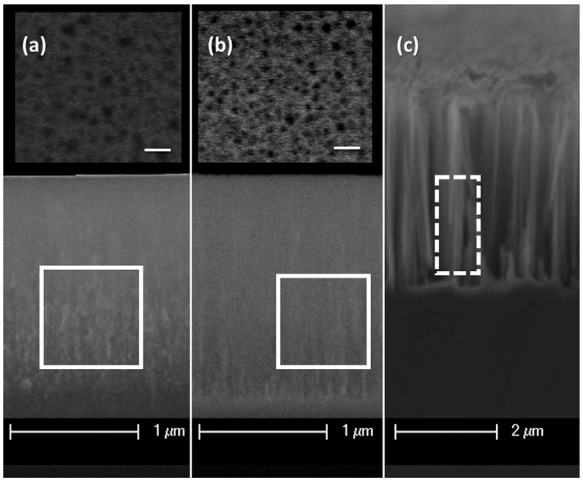

Fig. 1. Representative cross-section SEM images of (a) PSi Lo, (b) PSi Hi and (c) SiNW samples. The PSi samples have pore depths of 2 μm, while the SiNW has length of 3 μm. The white solid boxes highlight the disordered nanostructures in the PSi, while the white broken box highlights the uniform directionality of the NWs. Insets of (a) and (b) show the top view of the corresponding sample, with scale bars corresponding to 100 nm.

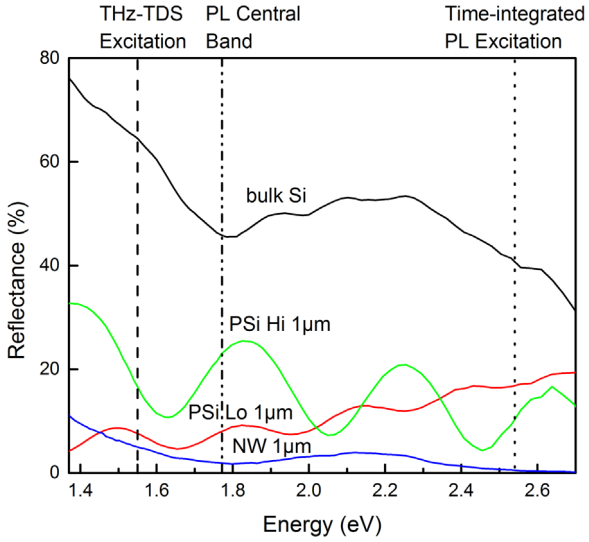

Fig. 2. Representative reflectance spectra of bulk, PSi and SiNW samples. The pore depths and NW thickness were 1 μm. The vertical dashed lines correspond to 1.55 eV, which is the excitation energy of the THz-TDS setup. The vertical dotted lines correspond to 2.54 eV, which is the excitation energy of the time-integrated PL setup. The vertical dashed-dotted lines correspond to the central PL bands at around 1.77 eV.